

# On the Canonical Proboscis

R. Finn and T. L. Leise

**Abstract.** It is proved that the "canonical proboscis" domains corresponding to prescribed contact angle  $\gamma_0$ , introduced in an earlier work by Fischer and Finn, are critical for the domain and angle, in the senses that (i) a solution of the capillary problem for angle  $\gamma$  in the absence of gravity exists over the domain if and only if  $\gamma$  is closer to  $\pi/2$  than is  $\gamma_0$ , and (ii) singular behavior at  $\gamma = \gamma_0$  occurs precisely over the proboscis portion of the domain. The construction can be effected in a continuum of ways, allowing the proboscis to occupy as large a portion of the domain as desired.

**Keywords:** *Capillarity, contact angle, mean curvature, canonical proboscis, subsidiary variational problem*

**AMS subject classification:** 76B45, 53A10, 49Q10

## 1. Background remarks

In 1974, Concus and Finn [2] proved a discontinuous dependence on boundary data of solutions to the "capillary problem" that are graphs over domains  $\Omega$  with protruding, locally rectilinear, corners. Physically, such solutions represent capillary free-surface interfaces, in vertical cylindrical tubes  $Z$  of section  $\Omega$ , which meet the smooth parts of the walls of  $Z$  in a prescribed "contact angle"  $\gamma$ ,  $0 \leq \gamma \leq \pi$ . The physical conditions suffice to determine the surface uniquely among graphs over  $\Omega$ , and apparently also among all embedded surfaces constrained to the interior of  $Z$ , see [2, 9, 12] (see [11] for a counterexample when the latter restriction fails). The authors in [2] proved that in the presence of a gravity field directed vertically downward into the fluid, the (limiting) surface height at the vertex  $P$  of the corner jumps discontinuously to infinity as  $|\frac{\pi}{2} - \gamma|$  increases across the half angle  $\alpha$ . This circumstance was used, initially by Coburn [2, pp. 220 - 221] in a "kitchen sink" experiment, and later by Weislogel [5, p. 136] under more controlled conditions, to measure the contact angle of water with acrylic plastic to an accuracy that is unattainable by other current methods.

In the absence of gravity the discontinuous dependence becomes more pronounced, to the extent that the solution surface, which can remain bounded and smooth over  $\Omega$  up to the critical configuration  $\alpha = |\frac{\pi}{2} - \gamma|$ , fails to exist in the expected form when that point is crossed, see [1]. Physically, if  $0 < \alpha < \frac{\pi}{2} - \gamma$  the local attraction of the fluid to the walls exceeds a critical value, causing the fluid to disappear out to positive infinity in the edge; similarly, if  $0 < \alpha < \gamma - \frac{\pi}{2}$  the fluid will disappear to negative infinity in the edge. This striking behavior formed the

---

R. Finn: Stanford University, Mathematics Department, Stanford, CA 94305, USA

T. L. Leise: Texas A & M University, Mathem. Department, College Station, TX 77843, USA

basis for a proposal by Concus and Finn [4] to use the phenomenon as a basis for space experiments that would lead to a very precise measurement of contact angle for many different materials, and perhaps shed new light on the extent to which contact angle can be viewed as an intrinsic property of materials.

As pointed out in [4], although the procedure shows considerable promise for angles  $\gamma$  reasonably close to  $\pi/2$ , technical difficulties could arise when  $\gamma$  is close to 0 or  $\pi$ , for the reason that the fluid then fills out (or empties) only a very small region near the edge when the critical value is crossed, and the discontinuity could become difficult to observe. For this reason, the authors in [4] proposed for such cases a configuration bounded by two circular arcs of differing radii, leading to a "nearly discontinuous" behavior at a critical angle, which could suffice for an accurate measurement. An elaboration of that configuration, leading to more precisely defined "near discontinuities", was introduced and studied in detail by Fischer and Finn in [10]. The particular properties of that modification led in turn to the tentative introduction of "canonical proboscis" domains - - which are determined explicitly by a kind of global singular behavior - - as section  $\Omega$  for  $Z$ , see [10]. The calculations of [10] strongly suggested that such domains can be constructed, *a*) to yield a "near discontinuity" at any prescribed contact angle other than  $\pi/2$ , and *b*) so that the singular behavior occurs over a set of simple form that occupies as large a portion of  $\Omega$  as desired, thus facilitating easy experimental determination of the critical angle. More detailed and extensive computer calculations by Concus, Finn, and Zabihi [6] corroborated the prediction in particular cases; however until now a formal proof that applies to all configurations was lacking. In the present paper we prove the assertions; we obtain also as corollaries of our procedure explicit estimates on the geometrical configuration of the "canonical" base domains, which should be of general mathematical as well as of experimental interest.

## 2. General considerations

We focus attention on a semi-infinite cylindrical tube  $Z$  with (base) section  $\Omega$ , whose boundary  $\Sigma$  consists of a finite number of smooth arcs meeting at well-defined interior angles  $2\phi$ . A corner defined by such an intersection point is called *reentrant* if  $2\phi > \pi$ ; if  $2\phi < \pi$  we refer to a *protruding* corner. We seek capillary surfaces  $u(x,y)$  defined over  $\Omega$  in the absence of external (gravity) field, bounding with  $\Omega$  a (prescribed) finite volume  $V$  of fluid, and meeting the bounding walls over the smooth parts of  $\Sigma$  in a prescribed (constant) angle  $\gamma$ ,  $0 \leq \gamma \leq \pi$ . Any such surface is determined as a solution of the equation

$$\operatorname{div} Tu = 2H \quad (1)$$

in  $\Omega$ , with

$$Tu = \frac{\nabla u}{\sqrt{1 + |\nabla u|^2}} \quad (2)$$

and

$$2H = \frac{|\Sigma|}{|\Omega|} \cos \gamma \tag{3}$$

under the boundary condition

$$v \cdot Tu = \cos \gamma \tag{4}$$

on  $\Sigma$ , where  $v$  is the exterior unit normal on  $\Sigma$ . Whenever such a surface exists it is unique up to an additive constant, even among surfaces that do not project simply onto  $\Omega$ , see Vogel [12]. In what follows we may assume  $0 \leq \gamma \leq \pi/2$ ; the supplementary case  $\pi/2 < \gamma \leq \pi$  reduces to that one under the reflection  $u \rightarrow -u$ .

The conditions for existence of such surfaces can be characterized by the following definition and theorem, which are taken from [10]. The theorem is a consequence of results that are proved in [7] and in [8], Chapters 6 and 7:

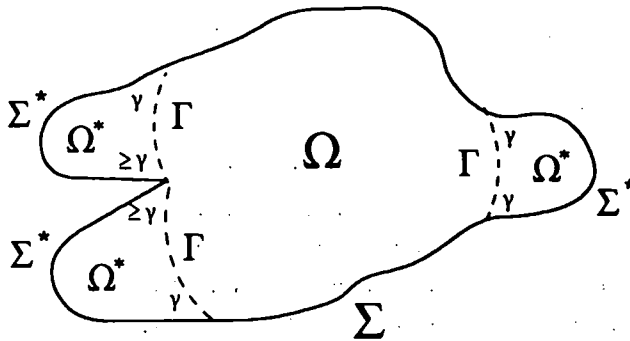


Figure 1. General domain  $\Omega$ ;  $\{\Gamma; \gamma\}$  configuration

**Definition:** A domain  $\Omega$  as above will be said to admit a  $\{\Gamma; \gamma\}$  configuration if there is a non-null proper subset  $\Omega^*$ , bounded in  $\Omega$  by a finite set  $\{\Gamma\}$  of subarcs of semicircles of radius  $R(\gamma) = \frac{1}{2H} = \frac{|\Omega|}{|\Sigma| \cos \gamma}$ , with the three properties:

- a) the  $\{\Gamma\}$  are disjoint except perhaps at reentrant corner points of  $\Sigma$ ,
- b) the curvature vector of each  $\Gamma$  is directed exterior to  $\Omega^*$ ,

c) each intersection point of any arc  $\Gamma \in \{\Gamma\}$  with  $\Sigma$  is either a reentrant corner with one sided angle between  $\Gamma$  and  $\Sigma$  not less than  $\gamma$  on the side of  $\Gamma$  opposite to its center and not less than  $\pi - \gamma$  on the other side, or else a point interior to a smooth subarc of  $\Sigma$  where  $\Gamma$  and  $\Sigma$  meet at angle  $\gamma$ .

An example of such a  $\{\Gamma; \gamma\}$  configuration is indicated in Figure 1. The arcs  $\Gamma$  appearing in the above definition are the *extremals* of a variational problem (for the functional  $\Phi$  below) “subsidiary” to the variational problem (principle of virtual work) giving rise to the original equation and boundary condition, see [8], Chapters 1 and 6. In general, extremal sets need not minimize. Additionally, they may not be uniquely determined; this circumstance is exploited in the considerations that follow.

**Theorem:** *A solution  $u(x,y)$  of problem (1)-(4) exists for given  $\Omega$  and  $\gamma \neq 0$  if and only if the functional*

$$\Phi = |\Gamma| - |\Sigma^*| \cos \gamma + \frac{1}{R} |\Omega^*| \tag{5}$$

*is positive for every  $\{\Gamma; \gamma\}$  configuration in  $\Omega$ . If  $\Phi \leq 0$  for any one such (non-null) configuration, then there exists one that minimizes  $\Phi$  among all such configurations.*

The case  $\gamma = 0$  requires special attention and will not be dealt with fully here.

### 3. The canonical proboscis

Following the procedure of [10], we seek to construct domains admitting an entire continuum of extremals, transforming into each other under parallel translation. According to the above remarks, for given contact angle  $\gamma_0$  the extremals  $\{\Gamma_0\}$  are circular arcs of common radius  $R_0$ , the value of which can be chosen arbitrarily in accordance with the scale invariance of the problem. We situate these arcs so that their centers are on the  $x$ -axis, and restrict attention to subarcs of the (semicircular) portions lying to the right of their centers. The condition that all arcs of the family meet the boundary  $\Sigma$  of  $\Omega$  in the same angle  $\gamma_0$  (interior to  $\Omega$  on the right of the arcs) leads to the equation

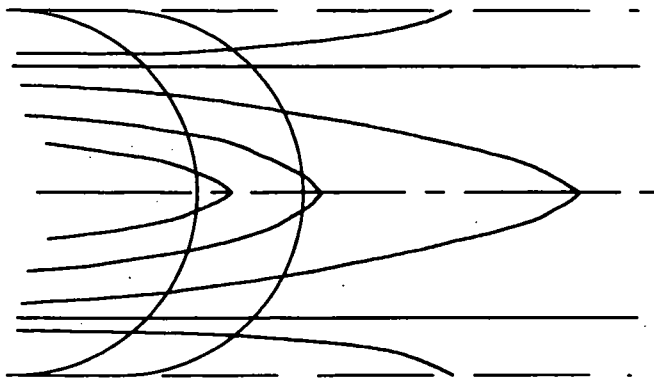


Figure 2. Extremal (circular) arcs, and integral curves (7) of (6)

$$\frac{dy}{dx} = \frac{y \sin \gamma_0 - \sqrt{R_0^2 - y^2} \cos \gamma_0}{y \cos \gamma_0 + \sqrt{R_0^2 - y^2} \sin \gamma_0} \tag{6}$$

for the portion  $\Sigma_0$  of  $\Sigma$  that meets the arcs, see [10]. This equation admits the family of explicit solutions

$$x + c = \sqrt{R_0^2 - y^2} + R_0^2 \sin \gamma_0 \ln \frac{\sqrt{R_0^2 - y^2} \cos \gamma_0 - y \sin \gamma_0}{R_0 + y \cos \gamma_0 + \sqrt{R_0^2 - y^2} \sin \gamma_0} \tag{7}$$

as represented in Figure 2 for a fixed  $\gamma_0$  and varying  $c$ . For purposes of the construction, only the curves between the two (trivial) solutions  $y = \pm R_0 \cos \gamma_0$  are of interest for us. These curves are shown in Figure 3 for six values of  $\gamma_0$  (decreasing upward), with the corresponding values of  $c$  adjusted to yield a common "vertex"  $P$  on the  $x$ -axis. Here the upper and lower branches intersect, according to the construction, in the angle  $2\alpha = \pi - 2\gamma_0$ .

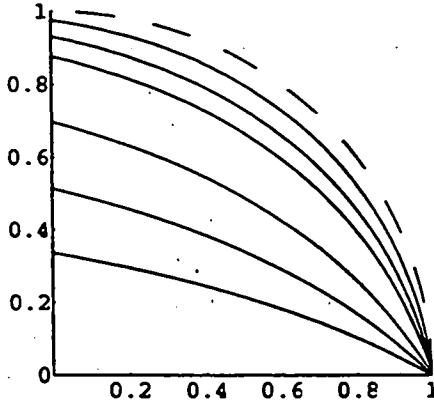


Figure 3. Upper halves of canonical proboscises:  $\gamma_0 = 60^\circ, 45^\circ, 30^\circ, 15^\circ, 10^\circ, 5^\circ, 0^\circ$

Proceeding as in [10], we now adjoin (symmetrically) a circular "bubble" of radius  $\rho$  at an arbitrarily chosen location on a pair of arcs corresponding to a prescribed  $\gamma_0$ , thus forming a closed domain  $\Omega_0$  as in Figure 4. It then follows from the above definition that the arcs  $\{\Gamma_0\}$  will be extremals for  $\Omega_0$  relative to the angle  $\gamma_0$  if and only if

$$R_0 = \frac{|\Omega_0|}{|\Sigma_0| \cos \gamma_0} \tag{8}$$

and it is not difficult to show that any such extremal is also extremal in the usual calculus of variations sense for the functional  $\Phi$ , cf. [8], Lemma 6.4. The equation (8) provides an implicit relation for the unknown radius  $\rho$ .

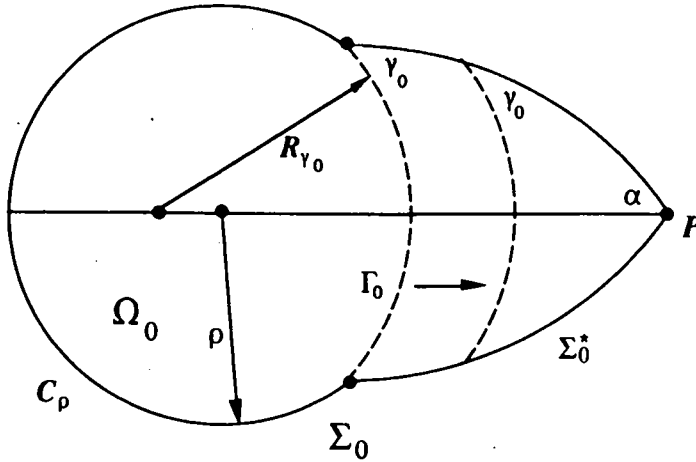


Figure 4. Canonical section, with proboscis

In [10] a value  $\rho$  yielding a solution for (8) was determined empirically, for various points of attachment. In the present paper we intend to prove the existence of a unique unbranched one parameter family of solutions containing the (uniquely determined) value  $\rho = 2 R_0 \cos \gamma_0$  that occurs when the attachment is at  $P$ , and to obtain meaningful upper and lower bounds for it.

We devote the following section to that material. We may assume that  $0 < \gamma < \pi/2$ . If  $\gamma > \pi/2$  we need only replace any given solution  $u(x,y)$  of (1) by its negative, which will have a contact angle in the indicated range. If  $\gamma = \pi/2$  the problem as we present it is improperly posed, however that case is accessible to the "wedge method" discussed in Section 1 above. We note that if  $\gamma = \pi/2$ , then problem (1) - (4) admits only the trivial solutions  $u = \text{constant}$ . The case  $\gamma = 0$  is singular in a different sense but can be studied directly, see below.

#### 4. Existence and radius bounds for canonical bubbles

Using (7) and (8) and the notation indicated in Figure 5, we can derive an equation relating  $\rho$  to  $\tau, \gamma_0$ , and  $R_0$ . From Figure 5 we see that on the upper half of the proboscis  $0 \leq y \leq R_0 \sin \tau$ . We note for later use that  $0 < \gamma_0 + \tau < \frac{\pi}{2}$ . The arclength of  $\Sigma_0$  is determined by integrating over  $\Sigma_0^*$  and then adding the result to the length of the circular arc  $C_\rho$  completing  $\Sigma_0$ :

$$\begin{aligned}
 |\Sigma_0| &= (2\pi - 2\beta)\rho + 2 \int_0^{R_0 \sin \tau} \sqrt{1 + \left(\frac{dx}{dy}\right)^2} dy \\
 &= (2\pi - 2\beta)\rho + 2 \int_0^{R_0 \sin \tau} \sqrt{1 + \left(\frac{y \cos \gamma_0 + \sqrt{R_0^2 - y^2} \sin \gamma_0}{y \sin \gamma_0 - \sqrt{R_0^2 - y^2} \cos \gamma_0}\right)^2} dy
 \end{aligned}$$

$$= (2\pi - 2\beta)\rho + 2R_0 \left( \sin \gamma_0 \ln \left( \frac{\cos \gamma_0}{\cos(\gamma_0 + \tau)} \right) + \tau \cos \gamma_0 \right).$$

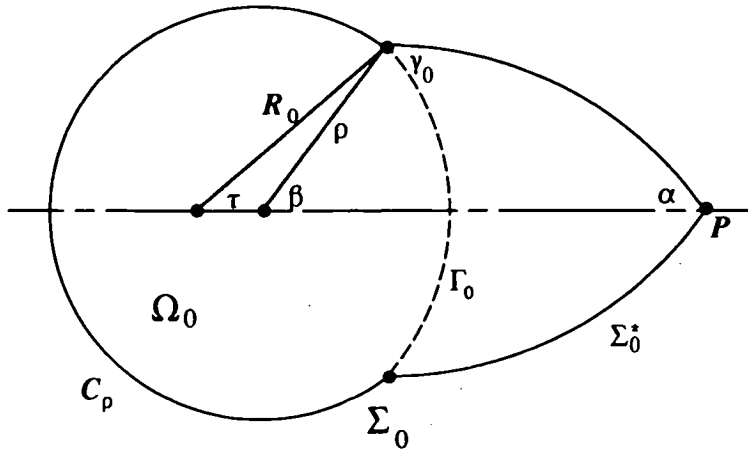


Figure 5. Relating  $\rho$  to  $R_0$ ,  $\gamma_0$  and  $\tau$

The area of  $\Omega_0$  is determined by integrating over the proboscis and then adding the result to the remaining circular area of  $\Omega_0$ :

$$\begin{aligned} |\Omega_0| &= (\pi - \beta + \sin \beta \cos \beta)\rho^2 - 2 \int_0^{R_0 \sin \tau} \frac{y}{y'} dy \\ &= (\pi - \beta + \sin \beta \cos \beta)\rho^2 - 2 \int_0^{R_0 \sin \tau} \frac{y^2 \cos \gamma_0 + y \sqrt{R_0^2 - y^2} \sin \gamma_0}{y \sin \gamma_0 - \sqrt{R_0^2 - y^2} \cos \gamma_0} dy \\ &= (\pi - \beta + \sin \beta \cos \beta)\rho^2 + R_0^2 \sin(2\gamma_0) \ln \left( \frac{\cos \gamma_0}{\cos(\gamma_0 + \tau)} \right) + \tau R_0^2 \cos(2\gamma_0) - \frac{1}{2} R_0^2 \sin(2\tau). \end{aligned}$$

Note that  $\beta$  depends on  $\rho$ ,  $\tau$ , and  $R_0$  and that the above equations hold whether  $\beta < \pi/2$  or  $\beta \geq \pi/2$ , see Figure 5.

Substituting into (8) we obtain

$$\begin{aligned} f(\tau, \beta, \rho; \gamma_0) &= (\pi - \beta + \sin \beta \cos \beta)\rho^2 - \tau R_0^2 \\ &\quad - R_0^2 \sin \tau \cos \tau - 2R_0 \rho (\pi - \beta) \cos \gamma_0 = 0. \end{aligned} \tag{9}$$

In order to remove  $\beta$  from (9) we first exclude the case  $\beta \geq \pi/2$ .

**Lemma 4.1:** *There exist no solution sets of (9) for which  $\rho > 0$ ,  $\beta \geq \pi/2$ ,  $0 < \tau < \pi/2$ ,  $0 < \gamma_0 < \pi/2$ , and  $R_0 > 0$ .*

**Proof:** In the case  $\beta \geq \frac{\pi}{2}$ , (9) becomes (see Fig. 5)

$$F(\tau, \rho; \gamma_0) = (2\rho R_0 \cos \gamma_0 - \rho^2) \sin^{-1} \left( \frac{R_0 \sin \tau}{\rho} \right) + \tau R_0^2 + R_0^2 \sin \tau \cos \tau + R_0 \sin \tau \sqrt{\rho^2 - R_0^2 \sin^2 \tau} = 0. \tag{10}$$

Suppose there were a solution set of (10) for which  $\rho > 0$ ,  $0 < \tau < \pi/2$ ,  $\beta \geq \pi/2$ ,  $0 < \gamma_0 < \pi/2$ , and  $R_0 > 0$ . All terms of (10) are nonnegative or strictly positive except  $(2\rho R_0 \cos \gamma_0 - \rho^2)$ , so necessarily  $\rho > 2R_0 \cos \gamma_0$ . Note that  $\cos \gamma_0 > \sin \tau$  due to the restrictions on  $\gamma_0$  and  $\tau$ . Now  $F(0, \rho; \gamma_0) = 0$  and if  $\beta \neq \pi/2$  then

$$\begin{aligned} \frac{\partial F}{\partial \tau} &= \frac{2R_0^2 \cos \tau}{\sqrt{\rho^2 - R_0^2 \sin^2 \tau}} (\rho \cos \gamma_0 - R_0 \sin^2 \tau) + 2R_0^2 \cos^2 \tau \\ &> \frac{2R_0^2 \cos \tau}{\sqrt{\rho^2 - R_0^2 \sin^2 \tau}} (2R_0 \cos^2 \gamma_0 - R_0 \sin^2 \tau) + 2R_0^2 \cos^2 \tau \\ &> 0. \end{aligned}$$

If  $\beta = \pi/2$  we find  $\frac{\partial F}{\partial \tau} = 2R_0^2 \cos^2 \tau > 0$ ; thus,  $F(\tau, \rho; \gamma_0) > 0$  for  $\tau > 0$ , a contradiction ■

We may thus assume that  $\beta < \pi/2$ . Using the relation  $R_0 \sin \tau = \rho \sin \beta$ , we obtain from (9)

$$F(\tau, \rho; \gamma_0) = \left( \pi - \sin^{-1} \left( \frac{R_0 \sin \tau}{\rho} \right) \right) (2\rho R_0 \cos \gamma_0 - \rho^2) + R_0^2 \tau + R_0^2 \sin \tau \cos \tau - R_0 \sin \tau \sqrt{\rho^2 - R_0^2 \sin^2 \tau} = 0. \tag{11}$$

This relation determines the radius  $\rho$  of the "bubble" that must be adjoined to the proboscis to guarantee that the circular arc meeting  $\Sigma_0^*$  will be extremal. We remark here the special case  $\gamma_0 = 0$ ,  $\tau = \pi/2$  which is not strictly included in the above discussion and which has a particular interest. Setting  $R_0 = 1$  and solving (11) yields the value 1.974... for  $\rho$ , which agrees with the value given in [3]. Although the procedure leads formally to a single extremal, the "keyhole configuration" (Figure 6) is obtained as an envelope of extremals. The length of the proboscis  $\Sigma_0^*$  in the figure can be chosen arbitrarily.

**Theorem 4.1:** *There exists a unique function  $\rho = \rho(\tau; \gamma_0)$  such that*

- i)  $\rho(0; \gamma_0) = 2R_0 \cos \gamma_0$ ,
- ii)  $\rho = \rho(\tau; \gamma_0)$  satisfies (11) on  $0 < \tau < \frac{\pi}{2} - \gamma_0$ , and
- iii)  $\rho = \rho(\tau; \gamma_0)$  is continuous, uniformly on  $0 \leq \tau < \frac{\pi}{2} - \gamma_0$ .



For this function, there holds

$$\text{iv) } R_0(\cos \gamma_0 + \min(\sin \gamma_0, \cos \gamma_0)) \leq \rho \leq 2R_0 .$$

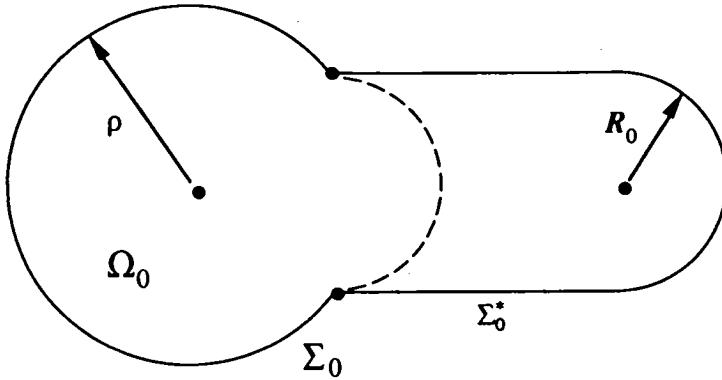


Figure 6. The keyhole configuration

(The relation  $\rho \leq 2 R_0$  was observed empirically in [10].)

**Proof:** We start by determining upper and lower bounds imposed by (11) on any such function.

**Lemma 4.2:** A function  $\rho = \rho(\tau; \gamma_0)$  satisfying i) - iii) satisfies also iv).

**Proof:** We consider first the range  $\rho = R_0(\cos \gamma_0 + \epsilon)$ ,  $0 \leq \epsilon \leq \cos \gamma_0$ , of which the right hand endpoint yields a solution of (11) corresponding to  $\tau = 0$ . If the indicated range is entered for some  $\tau > 0$ , we find from (11)

$$\begin{aligned} 0 &= \left( \pi - \sin^{-1} \left( \frac{\sin \tau}{\cos \gamma_0 + \epsilon} \right) \right) (\cos^2 \gamma_0 - \epsilon^2) + \sin \tau \cos \tau \\ &\quad + \tau - \sin \tau \sqrt{(\cos \gamma_0 + \epsilon)^2 - \sin^2 \tau} \\ &> \frac{\pi}{2} (\cos^2 \gamma_0 - \epsilon^2) + \sin \tau \cos \tau + \tau - \sin \tau (\cos \gamma_0 + \epsilon) \\ &> \frac{\pi}{2} (\cos^2 \gamma_0 - \epsilon^2) + \sin \tau (\cos \tau - \epsilon) . \end{aligned}$$

This relation fails if  $\epsilon = \min(\cos \gamma_0, \cos \tau)$ ; the left side of iv) thus follows from the observation that  $\cos \tau > \sin \gamma_0$ . On the other hand, suppose  $\rho = 2R_0$ . For  $\tau > 0$ , (11) now yields

$$\begin{aligned} F(\tau, 2R_0; \gamma_0) &= \left( \pi - \sin^{-1} \left( \frac{\sin \tau}{2} \right) \right) (4R_0^2 \cos \gamma_0 - 4R_0^2) \\ &\quad + R_0^2 \tau + R_0^2 \sin \tau \cos \tau - R_0^2 \sin \tau \sqrt{4 - \sin^2 \tau} = 0 . \end{aligned}$$

Since  $0 < \gamma_0 < \frac{\pi}{2}$ ,

$$\left( \pi - \sin^{-1} \left( \frac{\sin \tau}{2} \right) \right) (4 R_0^2 \cos \gamma_0 - 4 R_0^2) < 0.$$

Consider the remaining terms (with the  $R_0^2$  factored out):

$$g(\tau) = \tau + \sin \tau \cos \tau - \sin \tau \sqrt{4 - \sin^2 \tau}$$

$$\frac{dg}{d\tau} = 2 \cos^2 \tau - \cos \tau \sqrt{4 - \sin^2 \tau} + \frac{\sin^2 \tau \cos \tau}{\sqrt{4 - \sin^2 \tau}}$$

Note that  $g'(\pi/4) < 0$ . Suppose that there exists some  $\tau_0 > 0$  such that  $g'(\tau_0) = 0$ :

$$\begin{aligned} 2 \cos \tau_0 \sqrt{4 - \sin^2 \tau_0} - 4 + 2 \sin^2 \tau_0 &= 0 \\ 2 \cos \tau_0 - 2 + \sin^2 \tau_0 &> 0 \\ 2 \cos \tau_0 - \cos^2 \tau_0 &> 1. \end{aligned}$$

This is impossible since  $2 \cos \tau_0 - \cos^2 \tau_0 < 1$  for  $\tau_0 > 0$ . Thus  $dg/d\tau$  does not vanish on  $0 < \tau < \pi/2$ , so  $g'(\tau)$  must be negative on this interval. But  $g(0) = 0$ , and it follows that  $g(\tau) < 0$  for  $\tau > 0$ . There would follow  $F(\tau, 2R_0; \gamma_0) < 0$ , again contradicting the properties i), ii), iii) above ■

**Corollary 4.1:**  $\rho(\tau; \gamma_0) > R_0 \cos \gamma_0$  in  $0 \leq \tau < \frac{\pi}{2} - \gamma_0$ .

We are now prepared to complete the existence and uniqueness proof for the function  $\rho = \rho(\tau; \gamma_0)$ . In accordance with Lemma 4.2 we introduce

$$\begin{aligned} m_0 &= R_0 (\cos \gamma_0 + \min(\sin \gamma_0, \cos \gamma_0)) \\ M_0 &= 2 R_0. \end{aligned} \tag{12}$$

Let  $S$  be the set  $\{ \tau_0 \in [0, \frac{\pi}{2} - \gamma_0) : \exists ! \text{ function } \rho = \rho(\tau; \gamma_0) \text{ which satisfies i)-iii) and is defined for } \tau \in [0, \tau_0 + \varepsilon) \text{ for some } \varepsilon > 0 \}$ . We show that  $F_0$  is bounded below and  $F_\tau$  is bounded above in the region  $0 \leq \tau < \frac{\pi}{2} - \gamma_0$ ,  $m_0 \leq \rho < M_0$ :

$$\begin{aligned} |F_\tau| &= \left| 2 R_0^2 \cos^2 \tau + \frac{2 R_0^2 \cos \tau (R_0 \sin^2 \tau - \rho \cos \gamma_0)}{\sqrt{\rho^2 - R_0^2 \sin^2 \tau}} \right| \\ &\leq 2 R_0^2 \left( 1 + \left| \frac{R_0 \sin^2 \tau - \rho \cos \gamma_0}{\sqrt{\rho^2 - R_0^2 \sin^2 \tau}} \right| \right) \\ &\leq 2 R_0^2 \left( 1 + \frac{R_0 + M_0}{\sqrt{m_0^2 - R_0^2 \sin^2 \tau}} \right) \end{aligned}$$

since  $\rho > R_0 \cos \gamma_0 > R_0 \sin \tau$ , and

$$\begin{aligned} |F_\rho| &= \left| 2R_0 \cos \gamma_0 - 2\rho \left[ \pi - \sin^{-1} \frac{R_0 \sin \tau}{\rho} + \frac{R_0 \sin \tau}{\sqrt{\rho^2 - R_0^2 \sin^2 \tau}} \right] \right| \\ &= |2R_0 \cos \gamma_0 - 2\rho| |\pi - \beta + \tan \beta| \\ &\geq (2R_0 \min(\sin \gamma_0, \cos \gamma_0)) \left( \frac{\pi}{2} \right) \\ &= \pi R_0 \min(\sin \gamma_0, \cos \gamma_0). \end{aligned}$$

Therefore  $\rho(\tau; \gamma_0)$  has derivative  $\rho'(\tau) = -F_\rho / F_\tau$  which is continuous and bounded on  $S$ , for any  $\gamma_0 > 0$ . This result contains the assertion iii) above.

**Lemma 4.3:** For any  $\gamma_0 > 0$ ,  $S = [0, \tau^*)$ , where  $\tau^* = \text{lub} \{ \tau : \tau \in S \}$ .

**Proof:** For the initial value  $\rho(0; \gamma_0) = 2R_0 \cos \gamma_0$  there exists by the implicit function theorem for some  $\varepsilon > 0$  a unique continuous branch  $\rho = \rho(\tau; \gamma_0)$  satisfying (11) in  $0 \leq \tau < \varepsilon$ , in view of the estimates on  $F_\rho, F_\tau$  above. Thus  $0 \in S$ .

Let  $\tau_0 \in S$ . By the definition of  $S$ , there exists for some  $\varepsilon_0 > 0$  a unique continuous branch  $\rho = \rho(\tau; \gamma_0)$  satisfying the required conditions and defined on  $[0, \tau_0 + \varepsilon_0)$ . Therefore  $S$  is an open interval containing 0 in  $[0, \frac{\pi}{2} - \gamma_0)$ . From the definition of  $\tau^*$ , it follows that  $S = [0, \tau^*)$  ■

**Lemma 4.4:**  $S = [0, \frac{\pi}{2} - \gamma_0)$ .

**Proof:** Suppose  $\tau^* < \frac{\pi}{2} - \gamma_0$ . Define

$$\rho(\tau^*; \gamma_0) = \lim_{\tau \rightarrow \tau^*} \rho(\tau; \gamma_0) = \rho(0; \gamma_0) + \int_0^{\tau^*} \frac{d\rho}{d\tau} d\tau,$$

which limit exists since  $\rho'(\tau)$  is bounded in  $0 \leq \tau < \frac{\pi}{2} - \gamma_0$ . Clearly  $F$  and its derivatives are defined in the limiting configuration, and are continuous at  $\tau^*, \rho(\tau^*; \gamma_0)$ , hence by the implicit function theorem  $\rho$  could be extended past that point, contradicting the definition of  $\tau^*$ . This completes the proof of the lemma, and hence also of Theorem 4.1 ■

### 5. Canonical properties

There are two features to be noted in the above construction. One is that the (symmetric) points at which the "bubble" is attached to the solution curve of (6) can be chosen arbitrarily; that means that the "proboscis" portion of  $\Omega_0$  can be made as long (relative to the radius of the bubble) as desired, while it contains successively longer and wider rectangles as its length increases. This property is contained in Theorem 4.1. The other feature is that for any canonical proboscis, the angle  $\gamma_0$  is critical for the domain  $\Omega_0$  that has been determined, and that no extremals for that configuration and distinct from the  $\{\Gamma_0\}$  (see Figure 4) can appear. Precisely,

we have the following result:

**Theorem 5.1:** For any  $\gamma_0 \neq \pi/2$  and any canonical proboscis domain  $\Omega_0$  determined as above, there exists a solution of the capillary problem (1)-(4) in  $\Omega_0$  if and only if  $|\gamma - \frac{\pi}{2}| < |\gamma_0 - \frac{\pi}{2}|$ . If  $|\gamma - \frac{\pi}{2}| = |\gamma_0 - \frac{\pi}{2}|$  then every minimizing  $\{\Gamma; \gamma_0\}$  configuration for  $\Phi$  is determined by one of the arcs  $\Gamma_0$  indicated in Figure 4. That is, as  $|\gamma - \frac{\pi}{2}| \nearrow |\gamma_0 - \frac{\pi}{2}|$  the solution of (1)-(4) becomes singular exactly in the "proboscis" region swept out by the extremals  $\Gamma_0$ .

**Proof:** We may assume as above that  $\gamma, \gamma_0 < \pi/2$ . The case  $\gamma_0 = 0$  is covered in [2]. According to the theorem of Section 2, we need only show that if  $\frac{\pi}{2} - \gamma \leq \frac{\pi}{2} - \gamma_0 < \frac{\pi}{2}$  then there exists no  $\{\Gamma, \gamma\}$  configuration, distinct from the extremals  $\Gamma_0$  in the construction of the proboscis, for which  $\Phi \leq 0$ . According to Corollary 6.6, 6.7 of [8], it suffices to show that result in the particular case  $\gamma = \gamma_0$ . Were such a configuration to exist, there would have to be a minimizing one, by the theorem of Section 2. Since (as is easily shown) the  $\Phi$  functional is

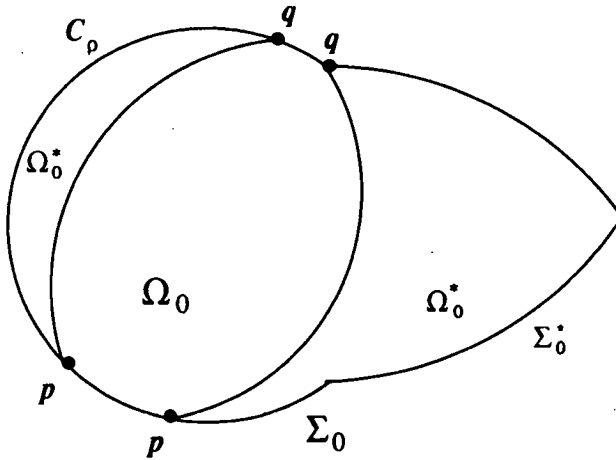


Figure 7. Cases 1 and 2

additive, there would have to be a single arc  $\Gamma$  that minimizes. Such an arc  $\Gamma$  would have radius  $R_0$  and would meet  $\Sigma = \partial\Omega$  either in the angle  $\gamma_0$  or else at a reentrant corner in a one sided angle not less than  $\gamma_0$ . We examine the various cases:

1.  $\Gamma$  meets the circular arc  $C_\rho$  of  $\Sigma$  at two interior points  $p$  and  $q$ , see Figure 7. This can only occur if  $\gamma_0 > 0$  and  $R_0 > \rho$ . Such a configuration would contradict the Corollary to Theorem 6.12 in [8].

2.  $\Gamma$  meets  $C_\rho$  at an interior point  $p$  and a reentrant corner  $q$ , see Figure 7. A small rotation of  $\Gamma$  about the center of  $C_\rho$  changes the geometry to the preceding case without

changing  $\phi$ . We thus obtain a contradiction as in Case 1.

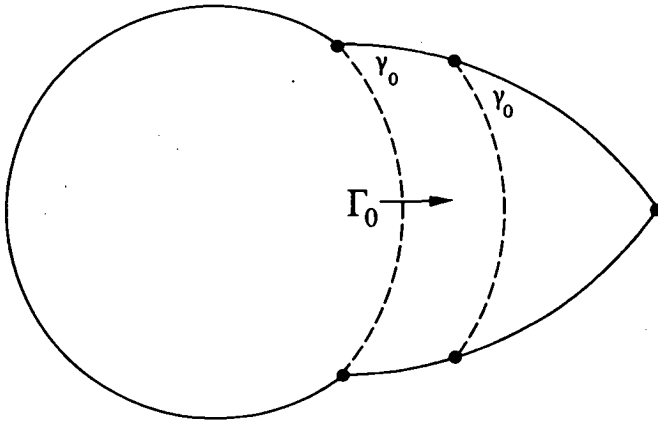


Figure 8. Case 3

3.  $\Gamma$  meets  $\Sigma_0$  at points  $p$  and  $q$ , each of which is either an interior point of the proboscis or a reentrant corner, with sense of curvature as in Figure 8. By construction of the proboscis,  $\Gamma$  must be contained in the continuum of extremals generated by translation of  $\Gamma_0$ .

This also excludes cases for which  $p$  and  $q$  are both on the upper half or both on the lower half of the proboscis.

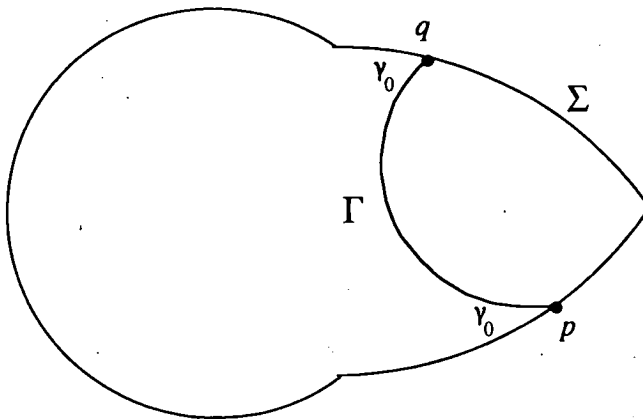


Figure 9. Case 4

4.  $\Gamma$  meets two interior points  $p$  and  $q$  of the proboscis, with sense of curvature as in Figure 9. We introduce the vertical segment joining  $q$  to  $p_0$  below it, and the extremal  $\Gamma_0$  of the generating family, that joins  $q$  to  $p_0$  (Figure 9a). Since  $\Gamma$  and  $\Gamma_0$  have the same radius, we obtain the reflection of  $\Gamma_0$  in the vertical segment by rotating  $\Gamma$  rigidly backwards about  $q$ .

This rotation cannot increase the incident angle  $\gamma_0$  at  $q$ . Since  $\Gamma_0$  is extremal, it meets  $\Sigma$  in the incident angle  $\gamma_0$ . That is not possible, since the slope of  $\Sigma$  is negative at  $q$ .

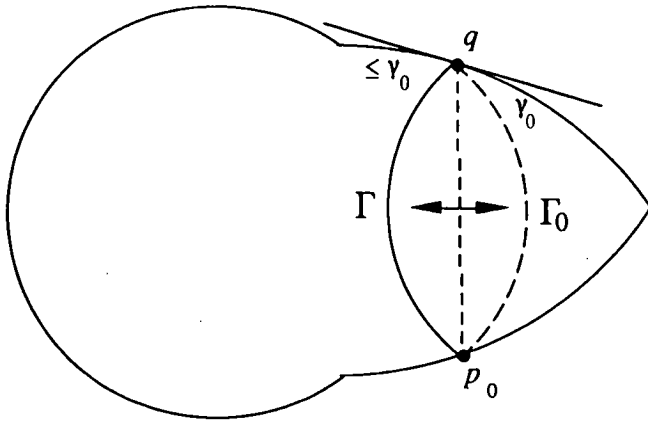


Figure 9a. Case 4 continued

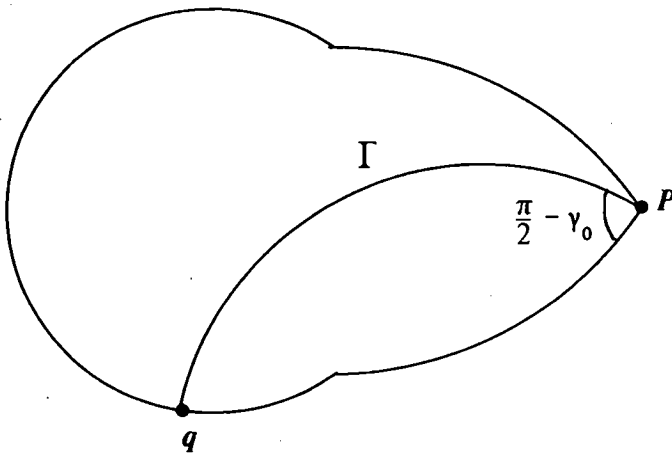


Figure 10. Case 5

5.  $\Gamma$  meets  $\Sigma_0$  at the tip  $P$  of the proboscis and another boundary point  $q$ , see Figure 10. By Theorem 6.10 of [8], no minimizing arc can meet  $\Sigma_0$  at a protruding corner; thus this case is excluded, since the opening angle at  $P$  is  $\pi - 2\gamma_0 < \pi$ .

6.  $\Gamma$  meets  $\Sigma_0$  at  $p$ , which is either an interior point of the proboscis or a reentrant corner, and a reentrant corner  $q$ , see Figure 11. This configuration is similar to Case 4 above, and we treat it analogously. We reflect the particular arc  $\Gamma_0$  that passes through  $q$  in the vertical through  $q$ , and we reflect also the tangent to the proboscis at  $q$ , obtaining locally the configuration shown in the inset of the figure. We thus find  $\sigma = \gamma_0 + 2\tau - \theta$ , where  $\theta \geq 0$  is the

angle obtained by rotating  $\Gamma$  until it coincides with the

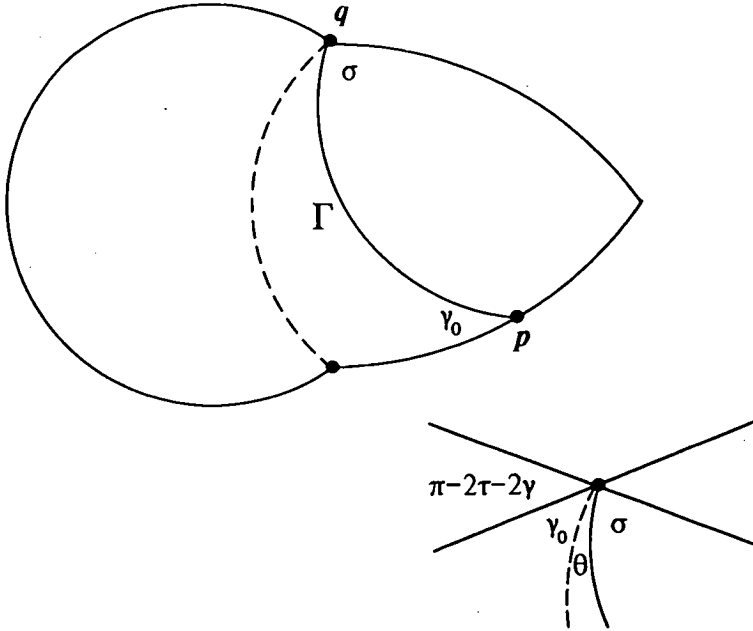


Figure 11. Case 6

reflection of  $\Gamma_0$ . By Theorem 6.10 of [8],  $\sigma \geq \pi - \gamma_0$ ; hence  $\gamma_0 + 2\tau - \theta \geq \pi - \gamma_0$ , from which  $\gamma_0 + \tau \geq \pi/2$ . This is a contradiction since  $\gamma_0 + \tau < \pi/2$  according to the construction in Section 3.

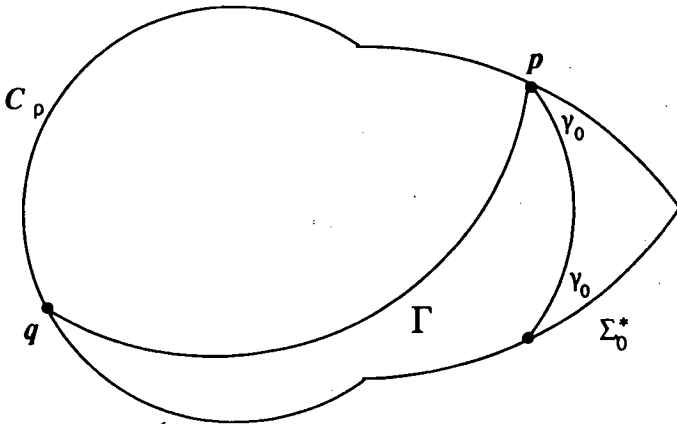


Figure 12. Case 7

7.  $\Gamma$  meets one interior point  $p$  of  $\Sigma_0^*$  and one interior point  $q$  of  $C_p$ , with sense of curvature as in Figure 12. This is excluded by the uniqueness of the extremals  $\{\Gamma_0\}$  through

the intersection points with  $\Sigma_0^*$ .

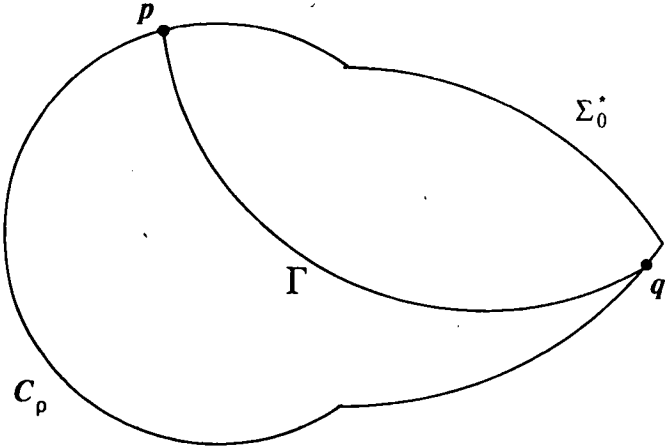


Figure 13. Case 8

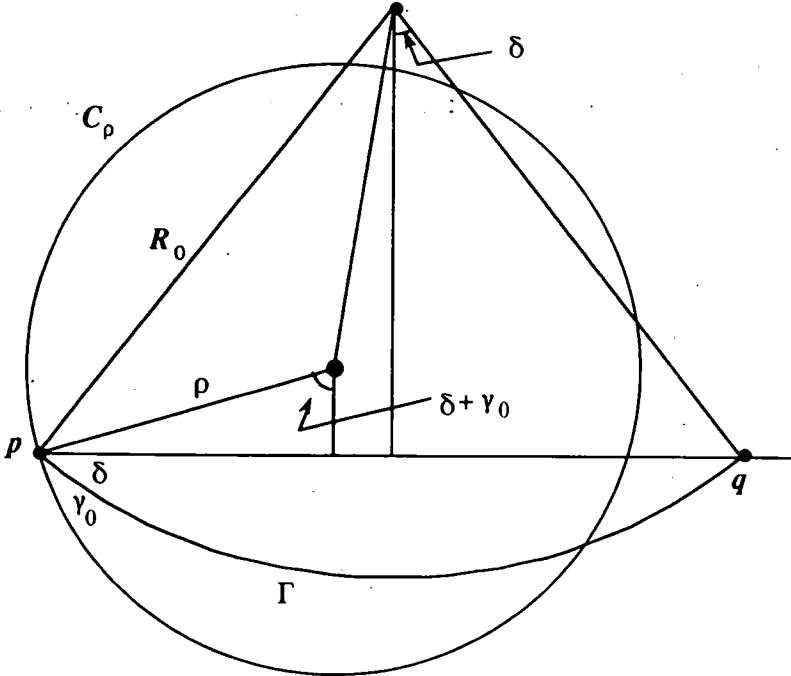


Figure 14. Case 8 continued



8.  $\Gamma$  meets one interior point  $p$  of  $\Sigma_0^*$  and one interior point  $q$  of  $C_\rho$  with sense of curvature as in Figure 13. With  $\delta$  defined as in Figure 14, suppose first that  $\gamma_0 + \delta \leq \pi/2$ . Figure 14 shows the configuration of Figure 13 rotated to put  $p$  and  $q$  at the same heights; the completed circle  $C_\rho$  is displayed and the proboscis shape suppressed for clarity. Since  $q$  is exterior to  $C_\rho$ ,  $\overline{pq}$  must have length exceeding  $2\rho \sin(\gamma + \delta)$ . But  $\overline{pq} = 2R_0 \sin \delta$ . There follows

$$\begin{aligned} R_0 \sin \delta &> \rho \sin(\gamma_0 + \delta) = \rho(\sin \gamma_0 \cos \delta + \cos \gamma_0 \sin \delta) \\ R_0 \cos \gamma_0 &> \rho(\sin \gamma_0 \cot \delta \cos \gamma_0 + \cos^2 \gamma_0) \\ &> \rho(\sin \gamma_0 \tan \gamma_0 \cos \gamma_0 + \cos^2 \gamma_0) \\ &= \rho \end{aligned}$$

which contradicts Corollary 4.1. Therefore  $\gamma_0 + \delta > \pi/2$ . By Theorem 6.16 of [8],  $\Gamma$  could then not minimize, a contradiction. Theorem 5.1 is proved ■

### 6. Some numerical examples

Figure 15 shows  $\rho/R_0$  as function of  $\tau$  for four values of  $\gamma$ . Note that the values do not change greatly for any  $\gamma$ , over the entire admissible range  $0 \leq \tau < \frac{\pi}{2} - \gamma$ , and that they remain within the bounds predicted by Lemma 4.2. Note also that monotonicity properties appear to reverse from small to large  $\gamma$ .

Figure 16 gives  $\rho/R_0$  as function of  $\gamma$  for fixed  $\tau$ . The lighter lines in the background show for comparison the function  $2\cos \gamma$  (the value of  $\rho/R_0$  at the initial value  $\tau = 0$ ), which is seen to provide a good approximation to the actual function.

Figure 17 is taken from [6] and shows computationally determined rise heights at  $P$  as function of contact angle  $\gamma$ , for proboscis domains of three different lengths (attachment points), in the case  $\gamma_0 = 30^\circ$ . The heights shown are relative to the height at the center of the attached "bubble". For comparison, the rise heights on the circumference, of the spherical cap solutions in a circular capillary tube of the same radius  $\rho$ , are shown as dotted lines. It is seen that although the fluid rise in the corner is not discontinuous as occurs for a planar wedge, the rise height in the proboscis is relatively small until  $\gamma$  becomes very close to  $\gamma_0$ , and then becomes extremely rapid. The proximity of  $\gamma$  to  $\gamma_0$  could thus be evidenced by sensors near the vertex point, at the top of a container of carefully chosen height. The method appears to open a prospect for contact angle measurements an order of magnitude more accurate than can be obtained with presently available procedures.

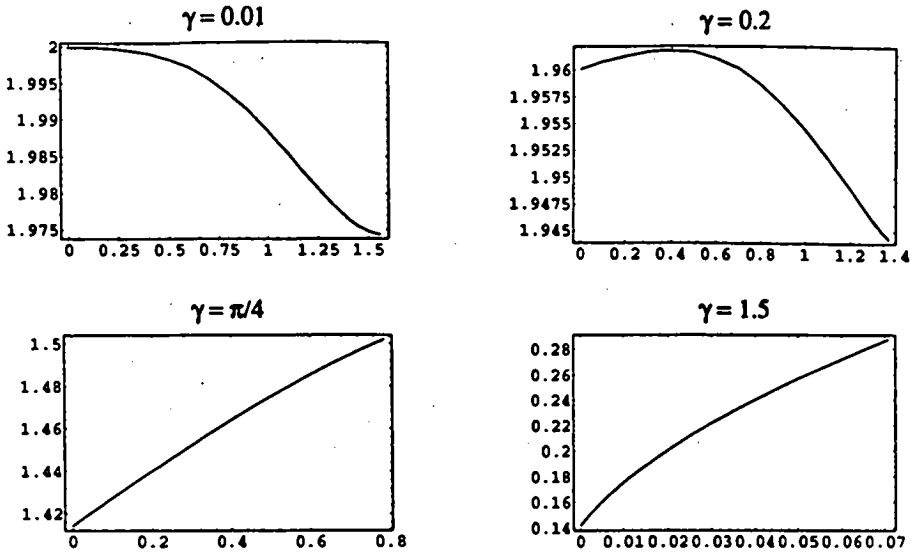


Figure 15. The function  $\frac{1}{R_0} \rho(\tau; \gamma_0)$  for  $\gamma_0$  as indicated

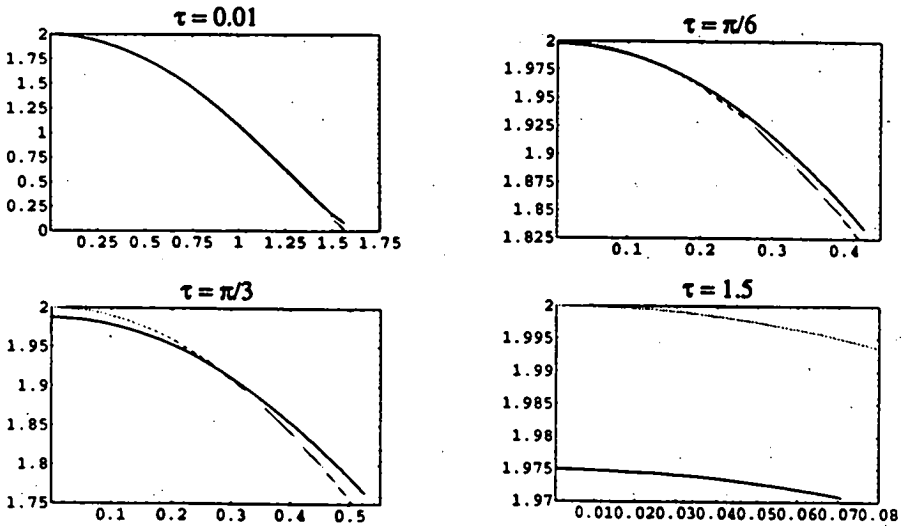


Figure 16.  $\frac{1}{R_0} \rho(\tau_0; \gamma)$  as a function of  $\gamma$  for  $\tau_0$  as indicated

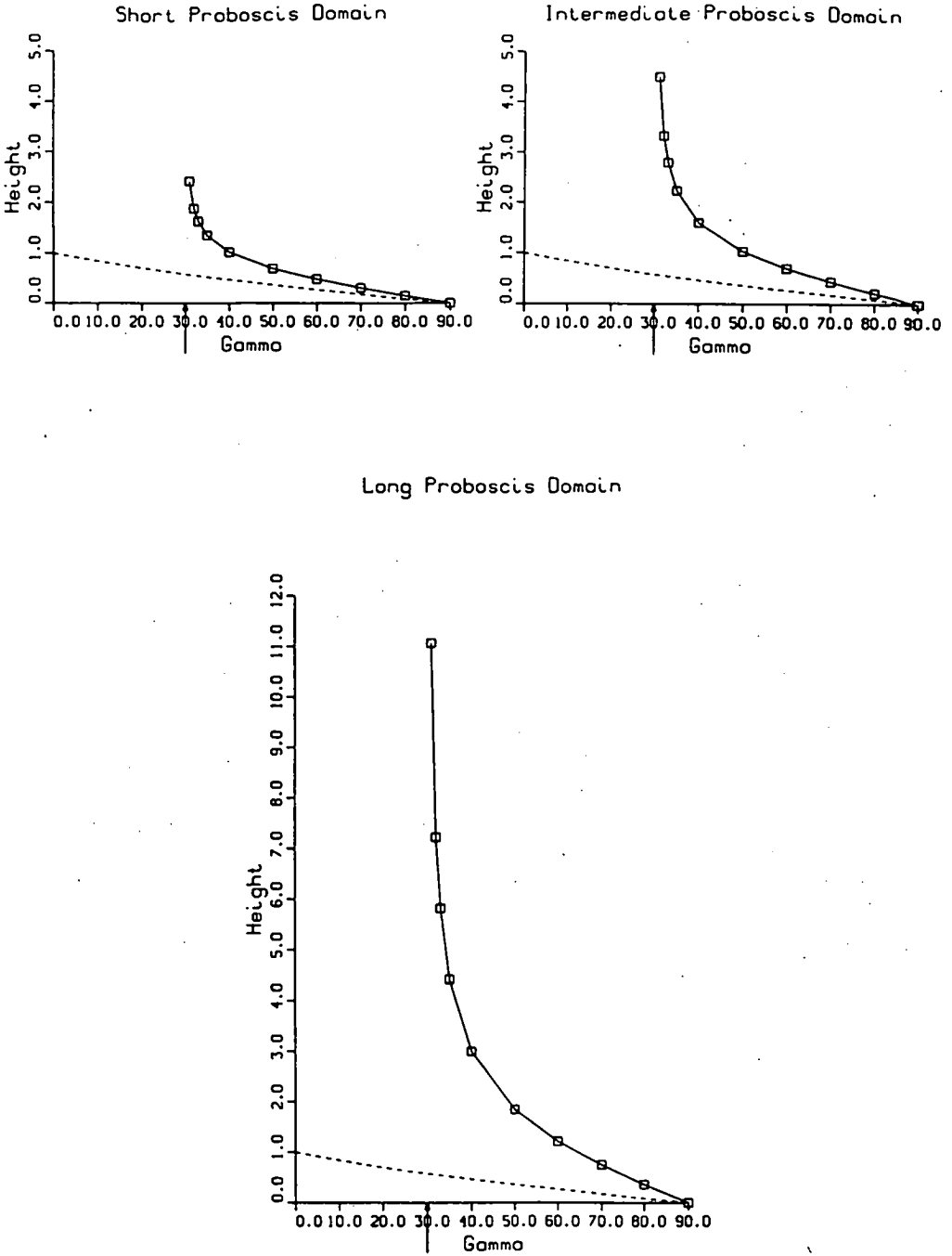


Figure 17. Rise height at  $P$  vs. contact angle for three canonical proboscises.  $\gamma_0 = 30^\circ$

This investigation was supported in part by a grant from the National Aeronautics and Space Administration, and in part by a grant from the National Science Foundation. The work was facilitated in part by the Undergraduate Research Opportunities Program at Stanford University.

## References

- [1] Concus, P. and R. Finn: *On capillary free surfaces in the absence of gravity*. Acta Math. 132 (1974), 177 - 198.
- [2] Concus, P. and R. Finn: *On capillary free surfaces in a gravitational field*. Acta Math. 132 (1974), 207 - 223.
- [3] Concus, P. and R. Finn: *Continuous and discontinuous disappearance of capillary surfaces*. In: Variational Methods for Free Surface Interfaces. Proc. Conf. 1985, Menlo Park/Calif., USA (eds.: P. Concus and R. Finn). New York et al.: Springer - Verlag 1987, pp. 197 - 204.
- [4] Concus, P. and R. Finn: *On accurate determination of contact angle*. In: Proc. IUTAM Symp. Micrograv. Fluid Mech., Bremen (ed.: H. J. Rath). New York: Springer - Verlag 1992, pp. 19 - 28.
- [5] Concus, P., Finn, R. and M. Weislogel: *Drop-tower experiments for capillary surfaces in an exotic container*. AIAA J. 30 (1992), 134 - 137.
- [6] Concus, P., Finn, R. and F. Zabihi: *On canonical cylinder sections for accurate determination of contact angle in microgravity*. In: Fluid Mechanics Phenomena in Microgravity (AMD: Vol. 154; eds.: D. A. Singer and M. M. Weislogel). New York: Amer. Soc. Mech. Engineers 1992, pp. 125 - 131.
- [7] Finn, R.: *A subsidiary variational problem and existence criteria for capillary surfaces*. J. reine ang. Math. 353 (1984), 196 - 214.
- [8] Finn, R.: *Equilibrium Capillary Surfaces*. New York: Springer - Verlag 1986.
- [9] Finn, R. and C. Gerhardt: *The internal sphere condition and the capillary problem*. Ann. Mat. Pura Appl. 112 (1977), 13 - 31.
- [10] Fischer, B. and R. Finn: *Non-existence theorems and measurement of capillary contact angle*. Z. Anal. Anw. 12 (1993), 405 - 423.
- [11] Hildebrandt, S. and F. Sauvigny: *Uniqueness of stable minimal surfaces with partially free boundaries*. J. Math. Soc. Japan (to appear).
- [12] Vogel, T. I: *Uniqueness for certain surfaces of prescribed mean curvature*. Pac. J. Math. 134 (1988), 197 - 207.

Received 14.12.1993